Clin Neuroradiol (2019) 29:27–36
https://doi.org/10.1007/s00062-017-0630-8

ORIGINAL ARTICLE

In vivo Metabolic Profiles as Determined by ^{31}P and short TE ^{1}H MR-Spectroscopy

No Difference Between Patients with IDH Wildtype and IDH Mutant Gliomas

Katharina J. Wenger[1,4] · Elke Hattingen[2,5] · Kea Franz[3] · Joachim Steinbach[1,4] · Oliver Bähr[1,4] · Ulrich Pilatus[2]

Received: 15 June 2017 / Accepted: 15 September 2017 / Published online: 5 October 2017

Abstract

Purpose Previous ex vivo spectroscopic data from tissue samples revealed differences in phospholipid metabolites between isocitrate dehydrogenase mutated (IDHmut) and IDH wildtype (IDHwt) gliomas. We investigated whether these changes can be found in vivo using ^{1}H-decoupled ^{31}P magnetic resonance spectroscopic imaging (MRSI) with 3D chemical shift imaging (CSI) at 3 T in patients with low and high-grade gliomas.

Methods The study included 33 prospectively enrolled, mostly untreated patients who met spectral quality criteria according to the World Health Organization (WHO II $n = 7$, WHO III $n = 17$, WHO IV $n = 9$; 25 patients IDHmut, 8 patients IDHwt). The MRSI protocol included ^{1}H decoupled ^{31}P MRSI with 3D CSI (3D ^{31}P CSI), 2D ^{1}H CSI and a ^{1}H single voxel spectroscopy sequence (TE 30 ms) from the tumor area. For ^{1}H MRS, absolute metabolite concentration values were calculated (phantom replacement method). For ^{31}P MRS, metabolite intensity ratios were calculated for the choline (C) and ethanolamine (E)-containing metabolites.

Results In our patient cohort we did not find significant differences for the ratio of phosphocholine (PC) and phosphoethanolamine (PE), PC/PE, ($p = 0.24$) for IDHmut compared to IDHwt gliomas. Furthermore, we found no elevated ratios of glycerophosphocholine (GPC) and glycerophosphoethanolamine (GPE), GPC/GPE, ($p = 0.68$) or GPC/PE ($p = 0.12$) for IDHmut gliomas. Even the ratio (PC+GPC)/(PE+GPE) showed no significant differences with respect to mutation status ($p = 0.16$). Nonetheless, changes related to tumor grade regarding intracellular pH (pH_i) and phospholipid metabolism as well as absolute metabolite concentrations of co-registered 2D ^{1}H CSI data for tumor and control tissue showed the anticipated results.

Conclusion Using 3D-CSI data acquisition, in vivo ^{31}P MR spectroscopic measurement of phospholipid metabolites could not distinguish between IDHmut and IDHwt.

Keywords MR Spectroscopy · Glioma · Mutations · IDH1 and IDH2 genes · Indirect detection

Oliver Bähr and Ulrich Pilatus contributed equally.

Electronic supplementary material The online version of this article (https://doi.org/10.1007/s00062-017-0630-8) contains supplementary material, which is available to authorized users.

✉ Elke Hattingen
elke.hattingen@ukbonn.de

1 Dr. Senckenberg Institute of Neurooncology, University Hospital Frankfurt, Goethe University, Frankfurt, Germany

2 Institute of Neuroradiology, University Hospital Frankfurt, Goethe University, Frankfurt, Germany

3 Department of Neurosurgery, University Hospital Frankfurt, Goethe University, Frankfurt, Germany

4 German Cancer Consortium (DKTK) and German Cancer Research Center (DKFZ), Heidelberg, Germany

5 Institute of Neuroradiology, University Hospital Bonn, Sigmund-Freud Straße 25, 53127 Bonn, Germany

Introduction

In 2016, the World Health Organization (WHO) classification of tumors of the central nervous system introduced molecular parameters in addition to histology to define primary brain tumors. Gliomas are now classified based on their morphologic appearance and on molecular markers, such as mutations in the isocitrate dehydrogenases isozyme 1 and 2 (IDH1 and IDH2) genes and a co-deletion of chromosomal arms 1p and 19q [1]. These changes led to a more accurate determination of prognosis and influence

treatment decisions. In addition, specific treatment options (targeted therapy) and biomarkers for treatment monitoring may arise from these genetic changes [2].

Mutations in the IDH1 gene occur in approximately 70% of WHO grades II–III gliomas and 80% of secondary glioblastomas (WHO IV) [3–5]. Mutations in the IDH2 gene are rare. Isocitrate dehydrogenases mutations are gain of function mutations as they catalyze the reduction of alpha-ketoglutarate (αKG) to the structurally similar metabolite 2-hydroxyglutarate (2-HG) [6, 7]. Tumor cells with IDH mutations contain over 100-fold more 2-HG compared to wildtype cells [7]. With this knowledge, a search for non-invasive options of 2-HG detection as a biomarker for the presence of IDH mutations was begun. So far no significant correlation between 2-HG levels in serum, cerebrospinal fluid (CSF) or urine with IDH mutation status has been found [8–10]. Several studies suggested that there is a positive correlation between 2-HG tissue levels and cell density, driving the hypothesis that cytoreductive therapy would lead to a decrease in 2-HG levels [11, 12] and 2-HG levels could therefore be used for therapy monitoring. Unfortunately, again prior research indicated that 2-HG serum levels of patients with IDH mutated gliomas (not discriminating between the two enantiomers), do not correlate with tumor volume obtained by fluid attenuated inversion recovery (FLAIR) imaging [9]. The same lack of correlation with tumor volume (T2/FLAIR) at the time of 2-HG sampling was found for urinary levels [10]. In conclusion, neither serum nor urinary levels are currently utilized to monitor treatment response.

Non-invasive Detection of 2-HG Using ^{1}H Magnetic Resonance Spectroscopy

It was considered as a breakthrough when 5 years ago, Andronesi et al. [14] and Choi et al. [15] reported the non-invasive in vivo detection of 2-HG in gliomas by ^{1}H magnetic resonance (MR) spectroscopy; however, the specific methods for quantitative detection of 2-HG are technically challenging. The signal pattern of the five non-exchangeable scalar-coupled protons of 2-HG is determined by multiplets which, depending on echo time, can lead to signal cancellation when further metabolites are present [13]. Especially for standard data acquisitions protocols (i. e. at TE of 30 ms) overlapping signals (mainly glutamate, glutamine, and gamma-aminobutyric acid [GABA]) can cause large errors in quantification of 2-HG concentrations [14, 15]. Despite these problems, first longitudinal observational studies have been published, monitoring 2-HG levels in untreated patients and patients undergoing standard therapy, showing a decrease in 2-HG concentration during treatment in serial imaging [16].

Detection of IDH Mutations Using ^{31}P MR-Spectroscopy

Another promising option for indirect non-invasive detection of IDH1 mutations in gliomas was presented in 2014, when Esmaeili et al. showed that mutated cells displayed a distinct profile of phospholipid metabolites compared to their wildtype counterparts [17]. They showed that IDH1 mutated gliomas have relatively higher glycerophosphocholine (GPC) and lower phosphoethanolamine (PE) tissue levels, resulting in more than two-fold higher phosphocholine (PC)/PE, GPC/glycerophosphoethanolamine (GPE), and GPC/PE ratios. The hypothesis of a distinct profile was evaluated using an E478 intracranial brain tumor xenograft model, containing a heterozygous IDH1-R132H mutation. In vivo ^{31}P MRS was performed on a preclinical 7T MR system operating at 121.7 MHz. It was later confirmed using ^{31}P HR-MAS MR looking at spectra of tissue extracts from an animal model as well as U251MG cell extracts expressing recombinant IDH1-R132H. Finally, samples of surgical biopsies from five patients with IDH wildtype WHO III–VI gliomas, one with a IDH wildtype WHO grade II glioma, four patients with IDH1-R132H WHO III–IV gliomas, and one with a IDH1-R132H WHO grade II glioma, were examined. The findings suggest that changes in phospholipid metabolism might offer an adequate method to discriminate and to monitor gliomas in respect to their IDH status; however, up to date, clinical translation is pending.

We tested the hypothesis that differences in phospholipid metabolites can discriminate between IDH1 mutated and wildtype gliomas in humans using in vivo ^{1}H decoupled ^{31}P MRSI applying 3D chemical shift imaging (3D-CSI).

Material and Methods

Study Design

At our institution, we enrolled 38 patients with mostly untreated grade II–IV gliomas in a prospective study, which included ^{1}H and ^{31}P MRS examinations. The IDH mutation status was determined by immunostaining (IDH1 R132H antibody) and Infinium Human Methylation 450 BeadChip analysis [18].

Results of the same study cohort focusing on ^{1}H MRS data for detection of 2-HG, are presented in a separate publication (submitted).

Magnetic Resonance Imaging

Measurements were performed on a clinical 3 T MR Scanner (Magnetom Trio, Siemens Medical Solutions, Erlangen, Germany) using a double-tuned ^{1}H/^{31}P volume head coil

(Rapid Biomedical, Rimpar, Germany). The MRI protocol included T2-weighted turbo spin echo MRI (3 orthogonal planes), a 3D gradient echo MRI sequence, ^{1}H decoupled ^{31}P MRSI with 3D chemical shift imaging (3D ^{31}P CSI), as well as 2D ^{1}H CSI. The ^{31}P sequence records the free induction decay (FID) following a 60° pulse excitation, applying a weighted circular phase encoding scheme in 3D (3D FID CSI). The pulse repetition time (TR) was 2000 ms. The matrix of 8 × 8 × 8 at 240 × 240 × 200 mm^3 field of view (FOV) was extrapolated to 16 × 16 × 16. During the first 30% of the data acquisition, ^{1}H decoupling was applied. For the center of the k-space 10 averages were obtained, leading to a total acquisition time of approximately 11 min. For 2D ^{1}H MRSI with a 2D Point-RESolved Spectroscopy (PRESS) sequence with circular weighted acquisition scheme was applied (matrix size 16 × 16, 12.5 mm slice thickness). The pulse repetition time was 1500 ms, the echo time 30 ms. Total acquisition time was approximately 5 min. Correct slab/slice placement was determined using three orthogonal planes. We additionally acquired two ^{1}H single voxel PRESS sequences at TE 30 ms and at TE 97 ms with 180° pulse spacing (as described by Choi et al. [15], typically with volumes of ≥ 8 ml) from the tumor area as defined on T2-weighted turbo spin echo. The results of ^{1}H single voxel PRESS TE 97 are the subject of a different publication and not reported here.

Data Analysis

Spectra of all ^{31}P and ^{1}H voxels were carefully reviewed for quality and spectra of insufficient quality (e.g. large line width, insufficient signal to noise ratio, and strong artifacts at visual inspection) were not included in the analysis. The ^{31}P MRSI data were analyzed in the time domain with advanced method for accurate, robust and efficient spectral (AMARES) fitting implemented in jMRUI (http://www.mrui.uab.es, version 4.0), while proton data were analyzed in the frequency domain with the software package LCModel (Provencher, version 6.3) [19]. Multimodal spectroscopic data were registered to 3D-anatomical data, employing an in-house software tool scripted in Matlab (The Mathworks, Natick, MA, USA), which allowed voxel selection on an MRSI grid overlay. Grid shift was applied where necessary. An area of interest within tumor tissue (center, unless necrosis or cyst) and control tissue on the contralateral hemisphere, was defined on T2-weighted turbo spin echo MRI data (slice thickness 4 mm, TR of 4340 ms, TE 10 ms) by an experienced neuroradiologist (EH, 10 years of experience in the field). Knowledge of previously acquired standard MRI images with gadolinium-based contrast agent was taken into account and voxel placement matched the area of the single voxel sequences.

As described by Hattingen et al. [20], the model fit for AMARES was composed of 14 exponentially decaying sinusoids. The signal of phosphocreatine (PCr) was adjusted to 0 ppm, and constraints for PC, PE, GPC and GPE signals were applied keeping the chemical shifts at a fixed difference with respect to the position of PCr while adjusting the line width to the value of PCr. A signal with a fixed chemical shift of 2.24 ppm and maximum line width of 50 Hz was used to account for potential macromolecule signals in the phosphodiester region. Another signal was used to model the signal of the inorganic phosphate (Pi) in the spectral region between 3.3 and 5.5 ppm. At physiological pH, H_2PO_4 and HPO_4 ions are known to contribute to the Pi signal. Since both components have a different chemical shift, the chemical shift δ0 (signal position) of inorganic phosphate (Pi) is pH dependent and can be used as a marker for intracellular pH (pH_i) [21, 22]. Following the approach by Petroff et al, [23], pH_i values of the predefined areas of the preselected voxels were determined from the chemical shift difference between Pi and PCr (pH = pkA + 10log ([δ1–δ0]/[δ0–δ2]). The formula is implemented in jMRUI with the default values pkA 6.75 ppm, δ1 3.27 ppm and δ2 5.63 ppm. Metabolite signal intensities were corrected for saturation effects caused by relaxation time T1, using previously published T1 relaxation times for ^{31}P metabolites from Hattingen et al. [24]. For statistical analysis, the following concentration ratios were calculated from the T1 corrected metabolite intensities: PC/PE, GPC/GPE, GPC/PE, PC/GPC, PE/GPE, (PC+GPC)/(PE+GPE).

The ^{1}H data were analyzed in the frequency domain using LCModel. For single voxel sequences at TE 30 ms, a three-dimensional volume-localized basis set was simulated using NMRScopeB [25]. The basis set included 2-HG, N-acetylaspartate (NAA), glutamate (Gln), creatine (Cr), glutamine (Glu), choline (Cho), myo-inositol (mI) and lactate (Lac). Short echo ^{1}H single voxel PRESS sequences (TE 30 ms) which provide improved shimming and higher signal-to-noise ratios (SNR), were specifically intended for analysis of Gln metabolism.

Individual metabolite values for ^{1}H MRS data NAA + NAAG, Cr and Cho were calculated using the phantom replacement technique described by Tofts and Grossman [26]. Correction factors for the signal loss caused by T1 and T2 at 3T were determined from previously published data for the reported metabolites [27]. The correction factor accounting for different coil loading (the respective transmitter reference amplitude) was considered on an individual patient basis.

Statistics

Statistical analysis was performed using commercially available software (STATISTICA, version 7.1; StatSoft,

Table 1 Patient characteristics

Characteristics	All patients for ^{31}P MRS analysis (n = 33)
General	
Age (years) median (range)	46.6 (26.7–78)
Female, (n)	60% (20)
Histology according to 2016 WHO classification of tumors of the central nervous system	
Glioblastoma, IDH wildtype, WHO IV (n)	18% (6)
Gliosarcoma, IDH wildtype, WHO IV (n)	3% (1)
Glioblastoma IDH mutant, WHO IV (n)	6% (2)
Anaplastic astrocytoma, IDH wildtype, WHO III (n)	3% (1)
Anaplastic astrocytoma, IDH mutant, WHO III (n)	30% (10)
Diffuse astrocytoma, IDH wildtype, WHO II	0% (0)
Diffuse astrocytoma, IDH mutant, WHO II (n)	9% (3)
Anaplastic oligodendroglioma, IDH mutant and 1p/19q codeleted, WHO III (n)	18% (6)
Oligodendroglioma, IDH mutant and 1p/19q codeleted, WHO II (n)	12% (4)
IDH mutation status	
IDH-1 R132H mutated (immunostaining) (n)	64% (21)
IDH-1 R132G mutated (sequencing) (n)	3% (1)
IDH-1 or IDH-2 mutated (450K methylation assay) (n)	9% (3)
IDH not mutated (immunostaining, 450K methylation assay) (n)	24% (8)
Prior treatment	
Patients with prior resection, (n)	6% (2)
Prior radiotherapy, (n)	3% (1)
Prior chemotherapy, (n)	3% (1)

Patient characteristics and prior treatment for the cohort are shown. The round half towards positive infinity rule is employed for all percentage values

Tulsa, OK, USA). Signal ratios for specific metabolites and absolute metabolite concentrations were analyzed with analysis of variance (ANOVA) comparing IDH1 and IDH2 mutated to IDH wildtype gliomas and high-grade (IV±III) to low-grade gliomas (II). Differences between tumor tissue and healthy control tissue were tested using ANOVA with repeated measurements. Results were considered to be significant at $p < 0.05$ by contrast analysis (t-test) in ANOVA. Tests were carried out only for specific metabolites and ratios with known alterations in mutated or malignant cells. Additional variants were not considered. We also applied a non-parametric test (Mann-Whitney U test) when comparing ^{31}P MRS detectable tumor metabolites between different patient cohorts.

Results

Patient Characteristics

Of the original patient cohort, three patients (8%) did not complete ^{31}P MRS scans, therefore no evaluable data was present. In two patients, IDH status was undefined (i. e. no histology, 5%), 33 patients could be included in the analysis of ^{31}P MRS data (WHO II n = 7, III n = 17, IV n = 9), 25 patients carried an IDH mutation (76%) and 8 patients were IDH wildtype (24%). For three patients, quality standards for ^{1}H CSI spectra were not met and data had to be excluded from analysis. The ^{1}H single voxel PRESS of tumor tissue was available for all but three patients, who did not complete the full MR examination. Of the patients included, two had received subtotal resection prior to enrolment, one had been treated with chemotherapy (temozolomide) and one with radiotherapy. Mean age at the time of enrolment was 46.6 (range 26.7–78) years and 60% of study subjects were female (n = 20). Patient characteristics are listed in Table 1. Representative ^{31}P MRS spectra for tumor tissue with and without IDH mutation at 3T are shown in Fig. 6.

Changes in Metabolism Related to IDH Mutation Status

In our patient cohort we did not find significant differences for the ratio of PC/PE (p = 0.24 t-test, p = 0.33 non-parametric) for IDH mutated compared to IDH wildtype gliomas. Glioblastomas exhibited an increased standard deviation (SD) with respect to PE (0.026 for WHO II compared to 0.056 for WHO IV; data extracted from Supplementary Table). A t-test performed comparing normalized

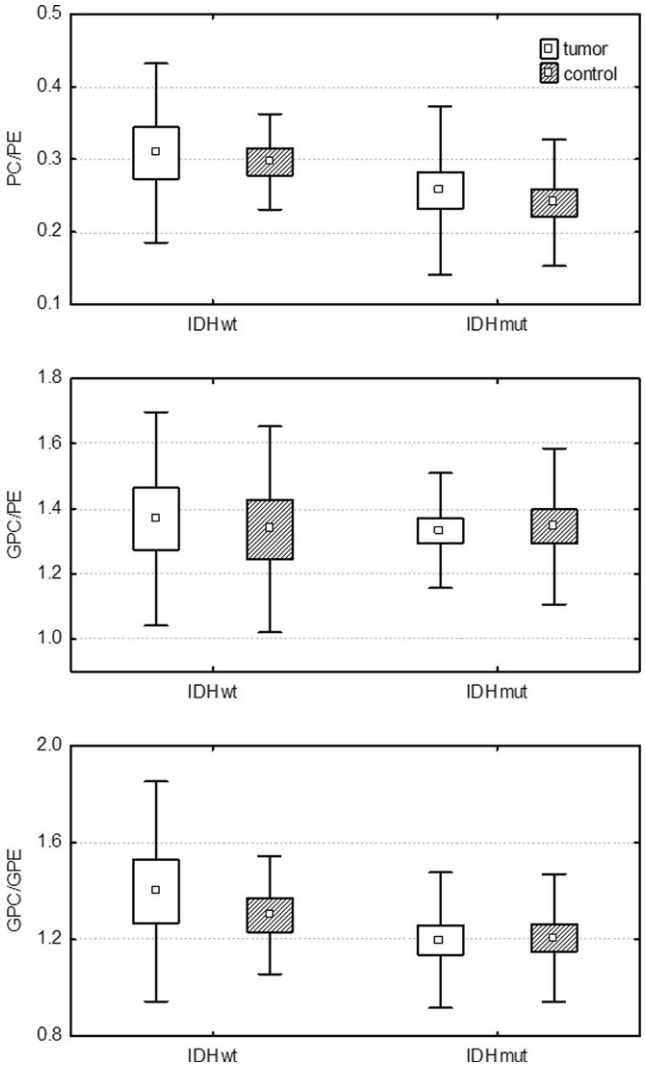

Fig. 1 Box-and-whisker plot. ^{1}H decoupled ^{31}P MRSI data with 3D chemical shift imaging (3D-CSI). Ratios of PC/PE, GPC/PE and GPC/GPE (y-axis) of IDH mutated ($n = 25$) compared to IDH wildtype glioma ($n = 8$; x-axis). Mean indicated within box. *Boxes* displaying standard error, *bars* representing standard deviation

PE for IDHmut to IDHwt (all tumor grades) revealed no significant difference or trend ($p = 0.59$). Furthermore, we found no elevated ratios of GPC/GPE ($p = 0.68$ t-test, $p = 0.76$ non-parametric) or GPC/PE ($p = 0.12$ t-test, $p = 0.14$ non-parametric) for IDH mutated gliomas (Fig. 1). Even the ratio of the sums of phosphocholine and glycerophosphocholine compounds (PC+GPC)/(PE+GPE) showed no significant differences with respect to mutation status ($p = 0.16$ t-test, $p = 0.14$ non-parametric, not shown). In addition, there were no significant differences for these ratios when correlating each compound with the respective value of normal appearing brain tissue (control) on an individual patient basis (i. e. $PC_{tumor}/PC_{control}$). Normalized signal intensities of the phospholipid metabolites are listed for tumor and control voxels for individual patients in the Supplementary Table. Looking at co-registered 2D ^{1}H CSI data with identical voxel placement, we did not find a depletion of NAA+NAAG for IDH mutated compared to IDH wildtype gliomas ($p = 0.89$) in our cohort. Comparing absolute metabolite concentrations (phantom replacement; mean) of Glu, Gln and Glu+Gln (Glx) of IDH mutated to IDH wildtype gliomas no significant difference was found for any of the metabolites (Fig. 2).

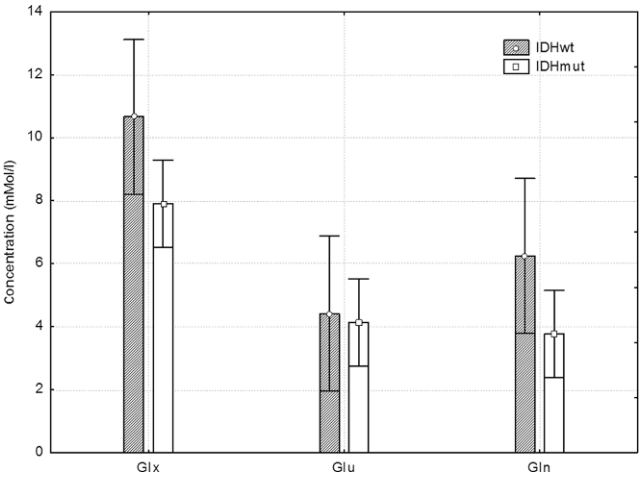

Fig. 2 Bar plot (mean) with standard deviation (SD) error bars. Absolute metabolite concentrations in mM (= mMol/l) obtained by short echo ^{1}H single voxel MRS (TE30; phantom replacement) of glutamate (Glu), glutamine (Gln) or Glu+Gln (Glx) comparing IDHmut ($n = 23$; *white boxes*) to IDHwt ($n = 7$; *striped boxes*) gliomas

Changes in Tumor pH_i

Considering tumor grade related changes, we did find a significantly higher pH_i (mean 7.11, SD = 0.08, $p < 0.001$) in tumor voxels of WHO IV gliomas, compared to control tissue (healthy tissue, contralateral hemisphere; mean 7.05, SD = 0.01). This increase in pH_i was also significant comparing tumor voxels of low grade gliomas (WHO II; mean 7.03, SD = 0.02) to respective voxels WHO IV gliomas (mean 7.11, SD = 0.08; $p < 0.001$ t-test; $p = 0.002$ non-parametric). Pooling WHO III and WHO IV gliomas, which are commonly considered as higher grade, significance was maintained ($p = 0.015$ t-test; $p = 0.018$ non-parametric).

Changes in Phospholipid Metabolism Related to Tumor Grade

We also calculated ratios of PC/GPC and PE/GPE, which have been previously reported to be elevated in recurrent glioblastoma tissue compared to control tissue [21], but no data for low-grade gliomas are available yet. The PC/GPC ratio showed no significant increase comparing low-grade gliomas (WHO II) to high-grade gliomas (WHO IV) ($p = 0.40$ t-test; $p = 0.46$ non-parametric). The PE/GPE showed

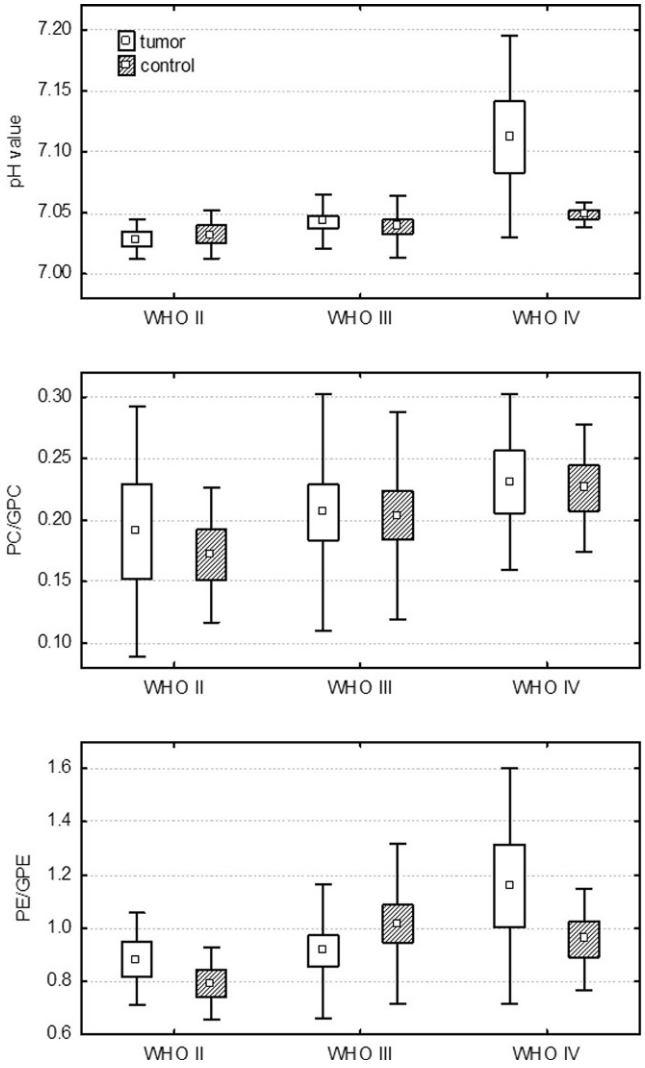

Fig. 3 Box-and-whisker plot. ^{1}H decoupled ^{31}P MRSI data with 3D chemical shift imaging (3D-CSI). Graphs show intracellular pH values, ratios of PC/GPC and PE/GPE in tumor tissue (*white boxes*) and control tissue (*striped boxes*) of WHO II, III and IV gliomas (WHO grade II $n = 7$, grade III $n = 17$, grade IV $n = 9$). Mean indicated within box. *Boxes* display standard error, *bars* represent standard deviation

a trend towards an increase comparing low-grade (WHO II) to high-grade gliomas (WHO IV; $p = 0.08$ t-test, $p = 0.15$ non-parametric), but failed to reach significance (Fig. 3). Representative spectral maps for pH_i and the ratio PE/GPE are shown for a patient with glioblastoma in Fig. 4.

General Changes in Metabolism Related to Tumor Grade

Metabolite concentration values in mM (= mMol/l) for coregistered 2D ^{1}H CSI data are listed in the Supplementary Table. High-grade gliomas (WHO IV) showed a significantly lower total creatine concentration (phosphocreatine+creatine; PCr+Cr) compared to control tissue (mean 4.61 vs. 6.51 mM, $p = 0.005$). There was a trend for a decrease of total creatine concentration in WHO III gliomas, but results failed to meet significance (mean 5.87 vs. 6.79 mM, $p = 0.07$). We could demonstrate a significant decrease of NAA+NAAG comparing tumor to control tissue for WHO II and III tumors (WHO II mean 4.76 vs. 7.92 mM, $p = 0.03$, WHO III mean 4.36 vs. 8.47 mM, $p < 0.001$). No significance was observed comparing tumor to control tissue in WHO IV gliomas (mean 5.87 vs. 8.31 mM, $p = 0.09$). Choline-containing compounds (Cho) showed a significant increase in WHO grade III and WHO grade IV gliomas compared to control tissue (WHO III mean 2.46 vs. 1.78 mM, $p = 0.007$; WHO IV mean 2.27 vs. 1.62 mM, $p = 0.05$). Total choline concentration was also elevated comparing tumor tissue of WHO II gliomas to WHO III and WHO IV. Significance was only reached relating WHO II to WHO III (1.62 vs. 2.46 mM, $p = 0.03$) (Fig. 5).

Discussion

Coregistered 2D ^{1}H CSI data with identical voxel placement showed the anticipated results in absolute metabolite concentrations with respect to tumor grade, even though tissue segmentation was not applied as voxel selection aimed to include only voxels filled entirely with tumor tissue. Results were in line with previously published data [28–31].

Depletion of NAA and NAAG has been shown for IDH1-mutated cells in vivo (tissue samples), resulting in lower mean levels of NAA and NAAG compared to tumors without IDH1 mutations. Current hypotheses are that N-acetyltransferase enzymes are down-regulated or that breakdown of N-acetylated amino acids is up-regulated [32]. This depletion was not confirmed in our in vivo data with a wide range of enrolled tumor grades and subtypes.

There was no significant difference for absolute metabolite concentrations (^{1}H single voxel; mean) of Glu, Gln or Glu+Gln (Glx) comparing IDH mutated to IDH wildtype gliomas. Fig. 2 only shows a minor trend towards Glx and Gln depletion in IDH mutated gliomas. Prior in vivo MRS studies have reported a significant decrease of pooled Glu and Gln [33] and HR-MAS studies reported decreased levels of Glu in IDH mutated glioma compared to wildtype [12].

In the in vivo ^{31}P MRS study we were not able to confirm the results of previous ex vivo studies which showed that the phospholipid profile from IDH mutated gliomas significantly differed from that in wildtype IDH gliomas [34]. We found no significant difference in ratios of PC/PE, GPC/GPE, GPC/PE or (PC+GPC)/(PE+GPE) for IDH mutated compared to IDH wildtype gliomas. If looking at Fig. 6 (representative ^{31}P MRS spectra for tumor tissue with and without IDH mutation at 3T) carefully, it can be seen

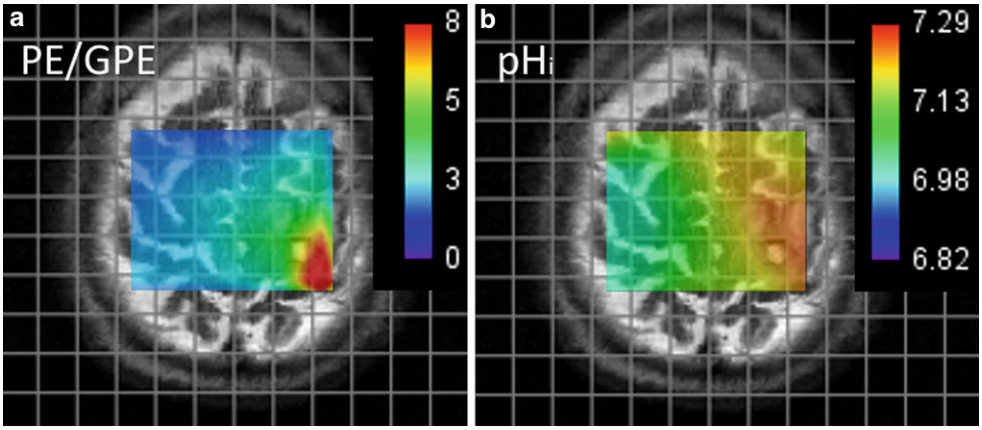

Fig. 4 Representative ^{31}P spectra registered to T2w anatomical data for the ratio PE/GPE (**a**) and pH_i (**b**) of a patient with glioblastoma (IDH wildtype) located in the left postcentral and precentral gyrus. Nominal matrix size of 8 × 8 × 8 was extrapolated to 16 × 16 × 16

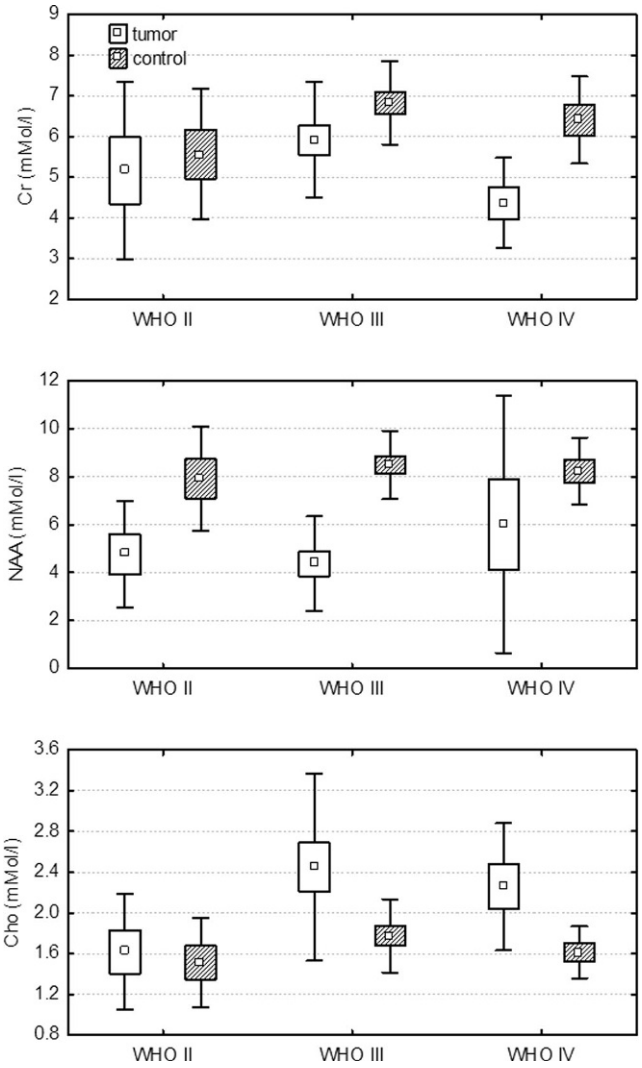

Fig. 5 Box-and-whisker plot. Metabolite concentration values in mM (= mMol/l) for coregistered 2D ^{1}H CSI data (phantom replacement) of total creatine concentration (Cr, phosphocreatine+creatine), choline-containing compounds (Cho) and NAA (NAA+NAAG) in tumor tissue (*white boxes*) and control tissue (*striped boxes*) of WHO II, III and IV gliomas (WHO grade II $n = 7$, grade III $n = 16$, grade IV $n = 7$). *Boxes* display standard error, *bars* represent standard deviation

that the spectral peaks of PE and PC of mutated tumor showed different patterns as those of nonmutated tumors. Since all but one patient in the IDHwt group were suffering from glioblastoma, this tumor grade was chosen for representative spectral data. In the IDHmut group, a patient with glioblastoma was specifically chosen for improved spectral comparison since there are tumor grade-related changes in phospholipid metabolism. Since glioblastomas exhibited an increased standard deviation (SD) with respect to PE and there was no significant difference or trend comparing normalized PE for IDHmut to IDHmut (all tumor grades), the obvious difference in the PE-region between the two exemplary shown cases in our opinion reflects the scattering between individuals for this specific compound in glioblastomas.

Choline and Ethanolamine Metabolism in IDH Mutated Gliomas

Esmaeili et al. [17] showed a significant decrease for the PE resonance and a significant increase for the GPC resonance of the IDH1-mutant E487 xenograft compared to the IDH1-wt xenografts (E473, E468, E434) in vivo and in tissue extracts. These changes translated to more than 2-fold higher than the above mentioned ratios in IDH1 mutant cells compared to wildtype. Of the ratios three (PC/PE, GPC/GPE, and PC+GPC)/(PE+GPE) were also significantly elevated in IDH mutated human glioma specimens. Changes were considered specific for IDH1 mutations since they were also evident in extracts of U251-MG cells stably overexpressing wildtype or mutant IDH1. The ^{31}P MRS in vivo experiments were performed on a preclinical 7 T MR system with a 3D MRSI pulse sequence with adiabatic excitation pulses. In vitro ^{31}P NMR spectra of tissue extracts were acquired on a 600 MHz spectrometer and high-resolution ^{31}P-MAS spectral tissue slices using a ^{1}H/^{31}C/^{31}P MAS probe on a 600 MHz spectrometer. Because of the relatively small sample sizes (for human specimens: 6 IDH wildtype gliomas WHO IV $n = 4$, WHO III $n = 1$, WHO II $n = 1$;

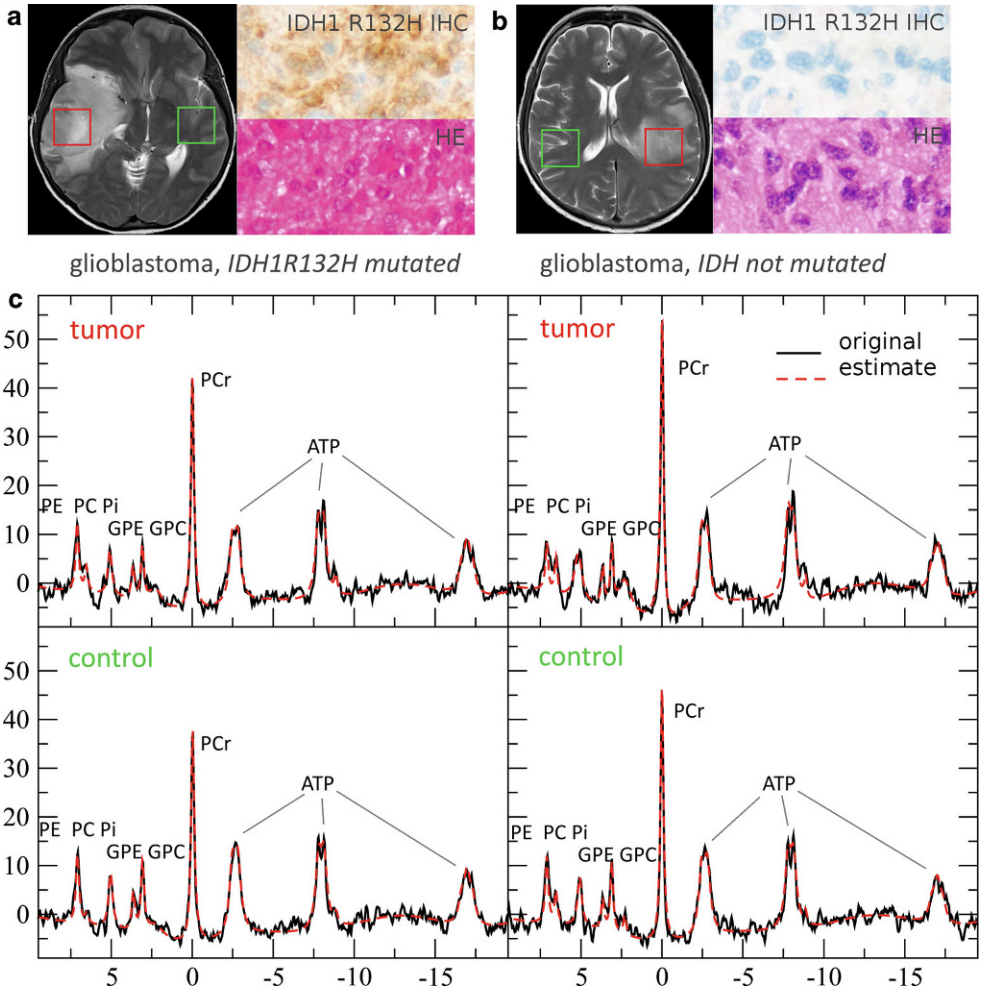

Fig. 6 Representative ^{31}P magnetic resonance spectra (MRS) for tumor tissue with and without IDH mutation at 3T. In the upper row (**a**, **b**) *green* (control) and *red* (tumor) *boxes* indicate voxel positioning on T2-weighted images while H&E staining and immunostaining of patient specimen with an antibody for mutant IDH1 (R132H) are shown to the right of the MR images. **c** shows the MRS data depicting the original spectrum as *black line* and the spectral fit, obtained as described in the methods section, as *red dotted line*. A WHO grade IV tumor was chosen as typical representative of an IDHwt tumor and was matched by an IDHmut tumor of the same grade for improved comparison. The figure may suggest a difference in the PC/PE ratio between the two exemplary shown cases, however, this reflects the scattering between individuals for this specific compound in glioblastomas

5 IDH1-R132H tumors WHO IV $n = 3$, WHO III $n = 1$, WHO II $n = 1$), an unpaired Mann-Whitney test was used. In another ^{1}H HR-MAS study (40 patients; WHO II $n = 14$, WHO III $n = 22$, WHO IV $n = 4$) Elkhaled et al. observed a correlation of GPC levels with increased 2-HG levels in IDH mutated tissue samples ($p = 0.003$). They also found a positive correlation for PC ($p = 0.003$) and PE levels ($p < 0.001$) with 2-HG [35]. The concomitant increase in PE will attenuate changes in the ratio and might explain why our study failed to show significant differences especially in ratios PC/PE and GPC/GPE between the two molecular groups.

With a different approach, based on a methylation analysis, Turcan et al. showed that the gene coding for choline kinase beta (CHKB) is hypermethylated in mutant IDH1 cells and the resulting transcriptional repression could account for a decrease in PC levels [36]. Without stratification of IDH mutation status, in 2009 Righi et al. showed that relative contributions of unphosphorylated choline, PC, and GPC to Cho were different for low (WHO II) and high grade (WHO III and IV) gliomas, using ^{1}H high-resolution magic angle spinning (HR-MAS, 11.7 T) in human biopsies [37]. They found GPC to be the main component of Cho in low-grade gliomas, whereas PC seems to be the dominant contribution to Cho in high-grade gliomas, which was confirmed by other studies [21, 38]. Statistically, more than 70% of WHO grade II and III gliomas are identified with IDH1R132H mutations; therefore, a pooling of WHO III and IV vs. WHO II gliomas does not allow a retrospective prognosis about a relationship of findings in phospholipid metabolism with IDH status.

With these partially contradictory results to date it remains unclear which exact mechanisms with respect to expression, post-translational modifications and cofactor levels affect enzyme activities in choline and ethanolamine metabolism in the presence of mutant IDH genes and how these mechanisms are related to tumor grade [34].

Study and Technical Limitations

Due to the sample size, we were not able to stratify for IDH mutated or IDH wildtype gliomas within WHO grading. Furthermore, partial volume effects of in vivo ^{31}P MRS at 3 T might have attenuated the metabolite changes. Com-

pared to the ^{1}H signal, the SNR ratio is low due to the relatively low sensitivity of the ^{31}P nucleus (1/16th of the ^{1}H nucleus). Even though larger tissue voxel volumes and more averages can partly compensate for low SNR, detection efficiency is still reduced by the fact that many molecules containing ^{31}P have short spin-spin (T2) relaxations times with a fast signal decay to baseline noise levels and long spin-lattice relaxation times (T1) with increased recovery times from repeated excitations. Larger voxel volumes and a 3D phase encoding scheme as a trade-off result in a poor spatial resolution [39]. The nominal matrix size before extrapolation in this and many other in vivo in human ^{31}P MRS studies is relatively small with 8 × 8 × 8 k-space sampling due to limited acquisition time within the protocol. This leads to an increased spreading of signal into adjacent voxels caused by the point spread function [40]. Despite the poor resolution we found significant changes in tumor pH_i compared to control tissue, which is due to changes in the expression/activity of plasma membrane ion transporters that facilitate proton efflux and enable tumor cells to maintain a higher intracellular pH [22]. Additionally, PE/GPE showed a trend towards an increase comparing low-grade to high-grade gliomas (p = 0.08). These results suggest that blurring due to poor resolution may not be the major confounding factor for our negative findings regarding the initial hypothesis.

Next to technical and study limitations, one remaining issue might be the heterogeneity of primary brain tumors with respect to tumor cell density. Heterogeneity is irrelevant for preclinical findings in cell cultures and less relevant for small localized sample volumes of stereotactic biopsies as used in the previous preclinical studies but gains relevance in large voxel volumes of ^{31}P MRS.

In conclusion, this in vivo ^{31}P MRS study failed to detect differences of phospholipid metabolite profiles between IDH mutated and wildtype human gliomas. A previous study with a small sample size including ex vivo spectroscopy of human glioma tissue, showed different metabolite profiles in respect to the IDH status. A larger sample size in our setting might detect differences in metabolic profiles, since the transfer of experimental MRS methods into human diagnostics often results in a loss of accuracy and requires compromises. Limited SNR of ^{31}P MRS at standard field strengths (1.5–3 T) requires a large voxel size to guarantee tolerable acquisition times. Large voxels however entail partial volume effects and artifacts which interfere with the metabolite spectra.

Funding Stiftung Tumorforschung Kopf-Hals (Wiesbaden, Germany), Frankfurter Forschungsförderung (Frankfurt, Germany).

Compliance with ethical guidelines

Conflict of interest K.J. Wenger, E. Hattingen, K. Franz, J. Steinbach, O. Bähr, and U. Pilatus declare that they have no competing interests.

Ethical standards All subjects gave written consent and the study was approved by the institutional review board (project number: SIN-04-2014).

References

1. Louis DN, Perry A, Reifenberger G, von Deimling A, Figarella-Branger D, Cavenee WK, Ohgaki H, Wiestler OD, Kleihues P, Ellison DW. The 2016 World Health Organization Classification of Tumors of the Central Nervous System: a summary. Acta Neuropathol. 2016;131:803–20.
2. Chen R, Cohen AL, Colman H. Targeted therapeutics in patients with high-grade gliomas: past, present, and future. Curr Treat Options Oncol. 2016;17:42.
3. Yan H, Parsons DW, Jin G, McLendon R, Rasheed BA, Yuan W, Kos I, Batinic-Haberle I, Jones S, Riggins GJ, Friedman H, Friedman A, Reardon D, Herndon J, Kinzler KW, Velculescu VE, Vogelstein B, Bigner DD. IDH1 and IDH2 mutations in gliomas. N Engl J Med. 2009;360:765–73.
4. Bleeker FE, Lamba S, Leenstra S, Troost D, Hulsebos T, Vandertop WP, Frattini M, Molinari F, Knowles M, Cerrato A, Rodolfo M, Scarpa A, Felicioni L, Buttitta F, Malatesta S, Marchetti A, Bardelli A. IDH1 mutations at residue p.R132 (IDH1(R132)) occur frequently in high-grade gliomas but not in other solid tumors. Hum Mutat. 2009;30:7–11.
5. Balss J, Meyer J, Mueller W, Korshunov A, Hartmann C, von Deimling A. Analysis of the IDH1 codon 132 mutation in brain tumors. Acta Neuropathol. 2008;116:597–602.
6. Watanabe T, Nobusawa S, Kleihues P, Ohgaki H. IDH1 mutations are early events in the development of astrocytomas and oligodendrogliomas. Am J Pathol. 2009;174:1149–53.
7. Dang L, White DW, Gross S, Bennett BD, Bittinger MA, Driggers EM, Fantin VR, Jang HG, Jin S, Keenan MC, Marks KM, Prins RM, Ward PS, Yen KE, Liau LM, Rabinowitz JD, Cantley LC, Thompson CB, Vander Heiden MG, Su SM. Cancer-associated IDH1 mutations produce 2-hydroxyglutarate. Nature. 2009;462:739–44.
8. Zhao H, Heimberger AB, Lu Z, Wu X, Hodges TR, Song R, Shen J. Metabolomics profiling in plasma samples from glioma patients correlates with tumor phenotypes. Oncotarget. 2016;7:20486–95.
9. Capper D, Simon M, Langhans CD, Okun JG, Tonn JC, Weller M, von Deimling A, Hartmann C; German Glioma Network. 2-Hydroxyglutarate concentration in serum from patients with gliomas does not correlate with IDH1/2 mutation status or tumor size. Int J Cancer. 2012;131:766–8.
10. Fathi AT, Nahed BV, Wander SA, Iafrate AJ, Borger DR, Hu R, Thabet A, Cahill DP, Perry AM, Joseph CP, Muzikansky A, Chi AS. Elevation of urinary 2-hydroxyglutarate in IDH-mutant glioma. Oncologist. 2016;21:214–9.
11. de la Fuente MI, Young RJ, Rubel J, Rosenblum M, Tisnado J, Briggs S, Arevalo-Perez J, Cross JR, Campos C, Straley K, Zhu D, Dong C, Thomas A, Omuro AA, Nolan CP, Pentsova E, Kaley TJ, Oh JH, Noeske R, Maher E, Choi C, Gutin PH, Holodny AI, Yen K, DeAngelis LM, Mellinghoff IK, Thakur SB. Integration of 2-hydroxyglutarate-proton magnetic resonance spectroscopy into clinical practice for disease monitoring in isocitrate dehydrogenase-mutant glioma. Neuro Oncol. 2016;18:283–90.

12. Jalbert LE, Elkhaled A, Phillips JJ, Neill E, Williams A, Crane JC, Olson MP, Molinaro AM, Berger MS, Kurhanewicz J, Ronen SM, Chang SM, Nelson SJ. Metabolic profiling of IDH mutation and malignant progression in infiltrating glioma. Sci Rep. 2017;7:44792.
13. de Graaf RA. In vivo NMR spectroscopy: principles and techniques. 2nd ed. Hoboken: Wiley; 2007.
14. Andronesi OC, Kim GS, Gerstner E, Batchelor T, Tzika AA, Fantin VR, Vander Heiden MG, Sorensen AG. Detection of 2-hydroxyglutarate in IDH-mutated glioma patients by in vivo spectral-editing and 2D correlation magnetic resonance spectroscopy. Sci Transl Med. 2012;4:116ra4.
15. Choi C, Ganji SK, DeBerardinis RJ, Hatanpaa KJ, Rakheja D, Kovacs Z, Yang XL, Mashimo T, Raisanen JM, Marin-Valencia I, Pascual JM, Madden CJ, Mickey BE, Malloy CR, Bachoo RM, Maher EA. 2-hydroxyglutarate detection by magnetic resonance spectroscopy in IDH-mutated patients with gliomas. Nat Med. 2012;18:624–9.
16. Choi C, Raisanen JM, Ganji SK, Zhang S, McNeil SS, An Z, Madan A, Hatanpaa KJ, Vemireddy V, Sheppard CA, Oliver D, Hulsey KM, Tiwari V, Mashimo T, Battiste J, Barnett S, Madden CJ, Patel TR, Pan E, Malloy CR, Mickey BE, Bachoo RM, Maher EA. Prospective longitudinal analysis of 2-hydroxyglutarate magnetic resonance spectroscopy identifies broad clinical utility for the management of patients with IDH-mutant Glioma. J Clin Oncol. 2016;34:4030–9.
17. Esmaeili M, Hamans BC, Navis AC, van Horssen R, Bathen TF, Gribbestad IS, Leenders WP, Heerschap A. IDH1 R132H mutation generates a distinct phospholipid metabolite profile in glioma. Cancer Res. 2014;74:4898–907.
18. Wiestler B, Capper D, Hovestadt V, Sill M, Jones DT, Hartmann C, Felsberg J, Platten M, Feiden W, Keyvani K, Pfister SM, Wiestler OD, Meyermann R, Reifenberger G, Pietsch T, von Deimling A, Weller M, Wick W. Assessing CpG island methylator phenotype, 1p/19q codeletion, and MGMT promoter methylation from epigenome-wide data in the biomarker cohort of the NOA-04 trial. Neuro Oncol. 2014;16:1630–8.
19. Provencher SW. Automatic quantitation of localized in vivo 1H spectra with LCModel. NMR Biomed. 2001;14:260–4.
20. Hattingen E, Magerkurth J, Pilatus U, Mozer A, Seifried C, Steinmetz H, Zanella F, Hilker R. Phosphorus and proton magnetic resonance spectroscopy demonstrates mitochondrial dysfunction in early and advanced Parkinson's disease. Brain. 2009;132:3285–97.
21. Hattingen E, Bähr O, Rieger J, Blasel S, Steinbach J, Pilatus U. Phospholipid metabolites in recurrent glioblastoma: in vivo markers detect different tumor phenotypes before and under antiangiogenic therapy. PLoS One. 2013;8(3):e56439.
22. Wenger KJ, Hattingen E, Franz K, Steinbach JP, Bähr O, Pilatus U. Intracellular pH measured by 31 P-MR-spectroscopy might predict site of progression in recurrent glioblastoma under antiangiogenic therapy. J Magn Reson Imaging. 2017;18:160.
23. Petroff OA, Prichard JW, Behar KL, Alger JR, den Hollander JA, Shulman RG. Cerebral intracellular pH by 31P nuclear magnetic resonance spectroscopy. Neurology. 1985;35:781–8.
24. Hattingen E, Magerkurth J, Pilatus U, Hübers A, Wahl M, Ziemann U. Combined (1)H and (31)P spectroscopy provides new insights into the pathobiochemistry of brain damage in multiple sclerosis. NMR Biomed. 2011;24:536–46.
25. Starčuk Z Jr, Starčuková J. Quantum-mechanical simulations for in vivo MR spectroscopy: principles and possibilities demonstrated with the program NMRscopeB. Anal Biochem. 2017;529:79-97.
26. Tofts P, Grossman RI. Quantitative MRI of the brain: measuring changes caused by disease. Hoboken: Wiley; 2004.
27. Hattingen E, Pilatus U, Franz K, Zanella FE, Lanfermann H. Evaluation of optimal echo time for 1H-spectroscopic imaging of brain tumors at 3 Tesla. J Magn Reson Imaging. 2007;26:427–31.
28. Herminghaus S, Pilatus U, Möller-Hartmann W, Raab P, Lanfermann H, Schlote W, Zanella FE. Increased choline levels coincide with enhanced proliferative activity of human neuroepithelial brain tumors. NMR Biomed. 2002;15:385–92.
29. Ishimaru H, Morikawa M, Iwanaga S, Kaminogo M, Ochi M, Hayashi K. Differentiation between high-grade glioma and metastatic brain tumor using single-voxel proton MR spectroscopy. Eur Radiol. 2001;11:1784–91.
30. McLean MA, Sun A, Bradstreet TE, Schaeffer AK, Liu H, Iannone R, Herman G, Railkar RA, Joubert I, Gillard JH, Price SJ, Griffiths JR. Repeatability of edited lactate and other metabolites in astrocytoma at 3T. J Magn Reson Imaging. 2012;36:468–75.
31. Rijpkema M, Schuuring J, van der Meulen Y, van der Graaf M, Bernsen H, Boerman R, van der Kogel A, Heerschap A. Characterization of oligodendrogliomas using short echo time 1H MR spectroscopic imaging. NMR Biomed. 2003;16:12–8.
32. Reitman ZJ, Jin G, Karoly ED, Spasojevic I, Yang J, Kinzler KW, He Y, Bigner DD, Vogelstein B, Yan H. Profiling the effects of isocitrate dehydrogenase 1 and 2 mutations on the cellular metabolome. Proc Natl Acad Sci U S A. 2011;108:3270–5.
33. Bisdas S, Chadzynski GL, Braun C, Schittenhelm J, Skardelly M, Hagberg GE, Ethofer T, Pohmann R, Shajan G, Engelmann J, Tabatabai G, Ziemann U, Ernemann U, Scheffler K. MR spectroscopy for in vivo assessment of the oncometabolite 2-hydroxyglutarate and its effects on cellular metabolism in human brain gliomas at 9.4T. J Magn Reson Imaging. 2016;44:823–33.
34. Izquierdo-Garcia JL, Viswanath P, Eriksson P, Chaumeil MM, Pieper RO, Phillips JJ, Ronen SM. Metabolic reprogramming in mutant IDH1 glioma cells. PLoS One. 2015;10(2):e0118781.
35. Elkhaled A, Jalbert LE, Phillips JJ, Yoshihara HAI, Parvataneni R, Srinivasan R, Bourne G, Berger MS, Chang SM, Cha S, Nelson SJ. Magnetic resonance of 2-hydroxyglutarate in IDH1-mutated low-grade gliomas. Sci Transl Med. 2012;4:116ra5.
36. Turcan S, Rohle D, Goenka A, Walsh LA, Fang F, Yilmaz E, Campos C, Fabius AW, Lu C, Ward PS, Thompson CB, Kaufman A, Guryanova O, Levine R, Heguy A, Viale A, Morris LG, Huse JT, Mellinghoff IK, Chan TA. IDH1 mutation is sufficient to establish the glioma hypermethylator phenotype. Nature. 2012;483:479–83.
37. Righi V, Roda JM, Paz J, Mucci A, Tugnoli V, Rodriguez-Tarduchy G, Barrios L, Schenetti L, Cerdán S, García-Martín ML. 1H HR-MAS and genomic analysis of human tumor biopsies discriminate between high and low grade astrocytomas. NMR Biomed. 2009;22:629–37.
38. Venkatesh HS, Chaumeil MM, Ward CS, Haas-Kogan DA, James CD, Ronen SM. Reduced phosphocholine and hyperpolarized lactate provide magnetic resonance biomarkers of PI3K/Akt/mTOR inhibition in glioblastoma. Neuro Oncol. 2012;14:315–25.
39. Bottomley PA, Griffiths JR, editors. Handbook of magnetic resonance spectroscopy in vivo: MRS theory, practice and applications. Chichester, Hoboken: Wiley & Sons; 2016.
40. Hattingen E, Pilatus U. Brain tumor imaging. Berlin: Springer; 2016.